Internal rotation arena: Program performances on the low barrier problem of 4-methylacetophenone

Sven Herbers, Oliver Zingsheim, Ha Vinh Lam Nguyen, Luis Bonah, Bettina Heyne, Nadine Wehres, Stephan Schlemmer

Internal rotation arena: Program performances on the low barrier problem of 4-methylacetophenone

Sven Herbers[a*], Oliver Zingsheim[b], Ha Vinh Lam Nguyen[c,d*], Luis Bonah[b], Bettina Heyne[b], Nadine Wehres[b], Stephan Schlemmer[b*]

[a] *Institute for Molecules and Materials, Radboud University,* Heijendaalseweg 135, NL-6525 AJ Nijmegen, Netherlands.
[b] *I. Physikalisches Institut, Universität zu Köln,* Zülpicher Straße 77, 50937 Köln, Germany
[c] *Univ Paris Est Creteil and Université de Paris, CNRS, LISA*, F-94010 Créteil, France
[d] *Institut Universitaire de France (IUF),* F-75231 Paris cedex 05, France
* Authors to whom correspondence should be addressed.
Email – Sven.herbers@science.ru.nl
Email – lam.nguyen@lisa.ipsl.fr
Email – Schlemmer@ph1.uni-koeln.de

Abstract: In the rotational spectroscopy community, several popular codes are available to treat multiple internal rotors in a molecule. In terms of the pros and the cons of each code, it often is a difficult task to decide which program to apply to a specific internal rotation problem. We faced this issue when dealing with the spectroscopic fingerprint of 4-methylacetophenone (4MAP), recently investigated in the microwave region, which we here extend into the millimeterwave region. The methyl group attached to the phenyl ring in 4MAP undergoes internal rotation with a very low barrier of only 22 cm^{-1}. The acetyl methyl group features a much higher barrier of about 580 cm^{-1}. The performances of a program using the so-called "local" approach in terms of Herschbach's perturbative treatment, *SPFIT*, as well as three programs *XIAM*, *ERHAM*, and *ntop*, representing "global" fits, were tested. The results aim at helping spectroscopists in the decision on how to tackle their own internal rotation problems.

1. Introduction

Internal rotation is an intramolecular, large amplitude motion (LAM), which causes all rotational lines to split into multiplets. The number of multiplet components depends on the quantity and fold number of internal rotors in the molecule. Rotational spectra of molecules featuring one or more internal rotors can no longer be treated with a semi-rigid rotor model. A Hamiltonian needs to be developed that addresses the specific internal degree of freedom, coupling to the overall rotation [1-3]. Model Hamiltonians dealing with internal rotation can then be implemented in programs, and many such programs are available, e.g., at the ''Programs for ROtational SPEctroscopy'' (PROSPE) website [4]. Among them, the *XIAM* code is particularly popular. It can deal with internal rotation effects of up to three rotors [5], though being somewhat limited with respect to available parameters. More flexible programs allow for the use of a much larger variety of parameters, e.g., the ones written by Groner, to treat up to two internal tops [6], by Kleiner, to treat a number of single-top [7,8] and two-top molecules [9] with C_s and C_1 symmetry, by Ilyushin, to deal with a single-top with C_s [10] and two-top molecules with C_{2v} symmetry [11], or the code developed by Ohashi and Hougen for methylamine-like molecules [12].

Internal rotation programs can be generally divided into four classes with the most important criterion being the coordinate system in which the Hamiltonian is defined: The Principal Axis Method (PAM), the Internal Axis Method (IAM), the ρ Axis Method (RAM), and the Combined Axis Method (CAM). It follows a short description of the different methods and associated programs.

PAM: The PAM works in the principal axis system, which is commonly used in pure rotational Hamiltonians. Only diagonal elements in the overall rotational moment of inertia tensor are non-zero. Some examples are the programs *aixPAM* [13], *ntop* [14], and *PAM-C2v-2tops* [11]. A version of the *BELGI* program, *BELGI-C_s-2Tops*, uses a slightly different method called "quasi-PAM" [9,15].

IAM: There is no explicit coupling between internal rotation and overall rotation in the IAM. One of the three reference axes is parallel to the coupling vector ρ, the other two axes rotate in dependence of the torsional angle α. Therefore, the moment of inertia tensor has off-diagonal elements and also depends on α, making the IAM method complicated to use, and there is no popular program set up in the IAM [2].

RAM: The RAM approximates the IAM with one axis parallel to the coupling vector ρ, but in contrast to the IAM, the coordinate system is fixed and does not rotate with α. Since the RAM does not work in the principal axis system, additional constants D_{ab}, D_{ac}, and D_{bc}, associated with the off-diagonal elements of the moment of inertia tensor, are inevitable. Programs working with the RAM are *BELGI* in its single-top version [7,8], *RAM36* [10], and the *IAMCALC/SPFIT* combination of programs [16] integrated into Pickett's *Calpgm* suite of programs [17]. None of these is commonly applied in the treatment of multiple rotors. Since the Hamiltonian is defined in the ρ axis system, the meaning of fitted parameters is often not as clear to the users, who are usually more familiar with the interpretation in the principal axis system. The codes are very flexible and a large number of fit parameters are available [10,16].

CAM: An approach combining the convenience of the PAM with the benefits of the RAM is the so-called Combined Axis Method (CAM) [18,19], as used in the program *XIAM* [5]. In a first step, the internal rotation is treated in the ρ axis system, and subsequently, a rotation matrix is used for a transformation into the principal axis system. An advantage of this method is the clear physical meaning

of internal rotation parameters used in the fits such as the barrier to internal rotation V_3, the reduced internal rotation constant F, and geometric angles δ and ε between the principal axes and the internal rotation axis, while providing rotational constants and centrifugal distortion coefficients in the principal axis system. An approach similar to the CAM is used in *ERHAM* [6,20] in the sense that there is a transformation between different axis systems. However, *ERHAM* treats the internal rotation in a quite different way, setting up matrix elements as Fourier series, and not explicitly solving the internal rotation Hamiltonian, which justifies giving *ERHAM* its own class [20]. An *ERHAM*-like treatment with *SPFIT* has been done, e.g., in the case of propane [21].

These different methods allow treatments with parameters shared between the different torsional species in terms of so-called global fits. However, it is also possible to carry out local fits with a set of independent parameters for each species. This is typically done by starting in the principal axis system and then proceeding in terms of Herschbach's perturbation treatment [22]. Here, each of the torsional species can be treated with their own "local" Hamiltonian:

$$H_{v\sigma} = H_{\mathrm{r}} + \sum_n W_{v\sigma}^{(n)} (\boldsymbol{\rho P})^n \qquad (1)$$

where H_{r} is the (semi) rigid rotor Hamiltonian, $\boldsymbol{\rho}$ is the coupling vector, whose absolute can have values between 0 (no coupling) and 1 (internal rotation and overall rotation are identical). The vector $\boldsymbol{P}$ is the angular momentum of the overall rotation. The series coefficients $W_{v\sigma}^{(n)}$, also known as Herschbach's barrier dependent perturbation coefficients for each torsional state v and symmetry species σ, depend on the reduced constant F of the internal rotor and on the reduced barrier $s = 4V_3/9F$ with V_3 being the barrier of a threefold periodic potential. Terms in the sum for uneven values of n are zero for the states in which σ is zero (A species) but non-zero for states with $\sigma = \pm 1$ (E species). Some values of $W_{v\sigma}^{(n)}$ in dependence of s are tabulated in Ref. [22].

Note that in the literature, the expression "local" often refers to different treatment of vibration-torsional states, but we will discuss only the vibrational ground state spectra. "Local" will thus refer to separate treatments of the symmetry species with no shared parameters, as can be done for example with the programs *SPFIT* [17] and *SFLAMS* [23]. Terms with even powers of n in the series of Eq. (1) can be incorporated in parameters of the semi-rigid rotor Hamiltonian. In this way, in particular the A species can be described solely by "effective" rotational parameters. For the E species, coefficients corresponding to the first order $n = 1$ terms

$$D_{\mathrm{g}} = F W_{v\sigma}^{(1)} \rho_{\mathrm{g}} \qquad \text{with g} = \mathrm{a, b, c}$$
$$\text{and } \rho_{\mathrm{g}} = \cos(\measuredangle \alpha, \mathrm{g}) I_\alpha / I_{\mathrm{g}} \qquad (2)$$

are often well-determined and can thus be used to derive the reduced barrier and geometric angles. I_α is the moment of inertia related to the methyl top, I_{g} are moments of inertia related to overall rotation. The angles $\measuredangle \alpha, \mathrm{g}$ are those between the internal rotation axis and the principal axes.

Eq. (1) works well for small values of ρ, apparent in the molecule 4-methylacetophenone (4MAP) of the present study. The two methyl groups in 4MAP, illustrated in Fig. 1, both undergo LAM. The *para*-methyl group attached to the ring features a very low

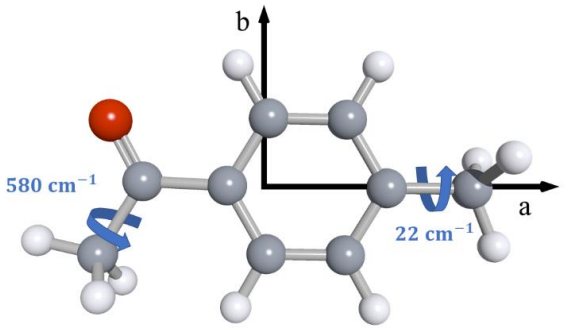

Figure 1. Geometry of 4MAP in its principal axis system optimized at the CAM-B3LYP/aug-cc-pVTZ level of theory. The hydrogen atoms are white, carbon atoms gray, and the oxygen atom is red. The barriers to internal rotation are 22 cm^{-1} (s = 1.77) for the lower barrier *para*-methyl and 580 cm^{-1} (s = 49) for the higher barrier acetyl methyl group.

torsional barrier of only 22 cm^{-1} and has a value of ρ = 0.022 associated with it. The acetyl methyl group has a much higher barrier of about 580 cm^{-1} and the absolute of the coupling vector is ρ = 0.015 [23].These small values of ρ make the series in Eq. (1) converge quickly due to the dependence on ρ^n. In contrast, this approach does not work for large values of ρ, typically found in small molecules composed of only a few atoms, like methanol with a value of ρ = 0.81 [24].

As briefly mentioned above and shown in some reviews on LAMs [1,2,25], each internal rotation program has its own advantages and drawbacks. The advantage of the CAM together with the user-friendly application of *XIAM* has made *XIAM* one of the most popular codes used in the spectroscopic community. A drawback of *XIAM* is its failure when it comes to low barrier cases observed in many previous studies [26-30] (s = 0.3 to 20.8), which was often claimed to be due to the negligence of interaction between the different torsional states [25].

In the previous microwave studies of 4MAP and studies on *m*-methylanisole, larger deviations in the *XIAM* fits were also observed. However, these deviations were traced back not to the negligence of interaction terms, but rather the limited amount of parameters available in the program [13,23,31]. Motivated by these findings, two additional parameters were implemented in the *XIAM* code, reproducing the chirped-pulse transition frequencies for 4MAP with J_{max} = 20 to measurement accuracy [23]. Results with similar accuracy were obtained with the program *ntop* working with the PAM [23]. Afterwards, the extended code, called *XIAM*$_{mod}$, was successfully applied on two other low barrier problems [32], but no attempts were made to test *XIAM*$_{mod}$ on torsional excited states, where for low barriers, near degenerate A species levels might cause additional problems.

Even in the ground state, some questions still remain in Ref. [23]. First, the data set is limited to relatively low J obtainable under the jet-cooled conditions and the performance of *XIAM*$_{mod}$ at high J is unknown so far. Second, local fits performed with *SFLAMS* in that study are unstable due to the small numbers of resolvable splittings arising from the high barrier acetyl methyl group which are close to the accuracy of 25 kHz of the spectrometer, and thus limit the predictive power of the fits. Finally, there are questions regarding the interpretability of the rotational constants obtained with *XIAM* in low barrier cases, as they might absorb internal rotation effects.

To answer these questions, we (i) extended the rotational spectrum of 4MAP to the millimeterwave (mmw) range recorded under room temperature to access high *J* data; (ii) recorded molecular jet Fourier transform spectra with an accuracy of about 5 kHz to resolve the torsional splittings arising from the acetyl methyl group for more rotational transitions; and (iii) compared the rotational constants obtained with different programs with respect to their interpretation as structural rotational constants.

2. Experimental Section

The dataset comprises a variety of experiments. One set of investigations was carried out on a cold molecular jet either in course of chirped pulse (expected accuracy about Δ*ν* = 25 kHz) or resonator measurements (Δ*ν* = 5 kHz). These experiments worked in the cm-wave region. The other set of experiments was carried out in a room temperature absorption cell in the mmw region (Δ*ν* = 50 kHz). The mmw experiments were sometimes aided with a double modulation scheme to properly identify weak signals. The given accuracies are used as line uncertainties in the fits.

2.1. Chirped-pulse Fourier transform microwave (CP-FTMW) spectrum (Δ*ν* = 25 kHz)

The microwave data from 8-18 GHz previously recorded at Purdue University [23] were extended by measurements in the range of 18-26.5 GHz using a broadband CP-FTMW spectrometer at the University of Cologne described in an earlier configuration in Ref. [33]. In the current configuration, the CP can be generated directly in the desired frequency range by a new arbitrary waveform generator (Keysight M8195A 65 GSa/s), which no longer requires mixing up the CP and mixing down the molecular signal. The substance was put on cotton wool and heated to 105°C in a reservoir screwed onto the General Valve Series 9 used in Ref. [33] to increase the vapor pressure. Neon was used as carrier gas at an absolute pressure of 1.5 bar. The measurement accuracy is estimated to be 25 kHz, similar to that of the Purdue spectra.

2.2. Resonator FTMW spectrum (Δ*ν* = 5 kHz)

Resonator measurements of selected signals between 2 and 26.5 GHz were recorded using a molecular jet FTMW spectrometer with a coaxially oriented beam-resonator arrangement (COBRA) described previously [34] to resolve torsional splittings of the high barrier rotor. The substance was kept in a steel tube in front of the nozzle and heated to 50°C. Helium as a carrier gas was allowed to stream at stagnation pressures of 1-2 bar over the sample before the helium-substance mixture was expanded into the resonator chamber.

2.3. Room temperature millimeter-wave absorption cell (Δ*ν* = 50 kHz)

The cooled molecular jet experiments were supported with data from room temperature absorption cell measurements using the frequency lock-in detection technique in the region of 76-119 GHz, carried out at Cologne University. The experimental scheme was described in detail before [35,36]. A 14 m long single path absorption cell with an approximate diameter of 10 cm was filled with 10 µbar of gaseous 4MAP. No heating was required. Due to the 2*f*-demodulation, absorption features appear close to a second derivative of a Voigt profile. Broadband scans were not viable because of inevitable long integration times. Hence, only parts of particular interest of the spectrum were recorded.

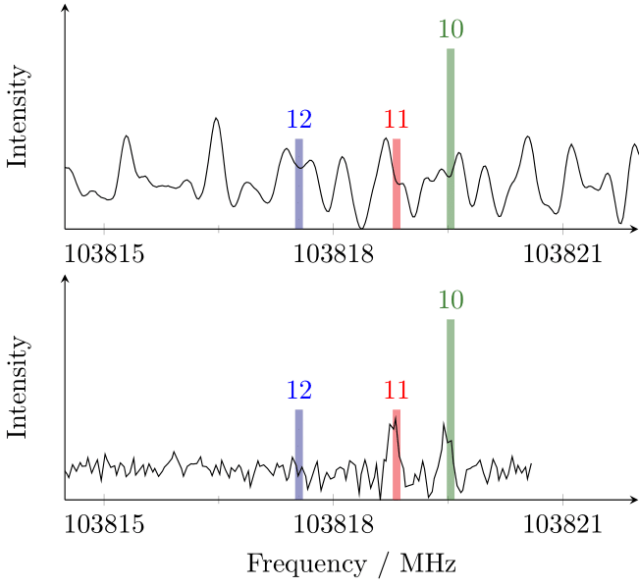

Figure 2. Upper trace: A section of the 2*f*-absorption mmw spectrum. The (10), (11), and (12) symmetry species of the $J'_{K'_a,K'_c}$←$J''_{K''_a,K''_c} = 84_{1,83} - 84_{0,84}$ transition predicted with the program *XIAM* are indicated as colored vertical lines. The spin statistical weight was considered [23]. As can be seen, no clear features are resolvable. Lower trace: The same portion of the spectrum in the double-modulation double-resonance experiment. The (12) component appears to be missing and is predicted by *ERHAM* to be degenerate with the (11). The pump transition was the degenerate pair of $85_{1,85} - 84_{1,84}$ and $85_{0,85} - 84_{0,84}$ at 111193.279 MHz, all three aforementioned symmetry species are degenerate for this pump transition.

For a few signals of interest, in particularly dense regions of the spectrum, double-modulation double-resonance (DM-DR) measurements were conducted with a second, more powerful (~60 mW) (pump-)radiation source, whose polarization is orthogonal to the probe beam (~1 mW) [37]. As a central feature of the DM-DR technique only probe transitions which share an energy level with the pump transition appear in the spectra. Therefore, the DM-DR spectrum pulls these specific transitions out of the plethora of transitions of a conventional absorption spectrum. These confusion- and baseline-free spectra dramatically simplify the analysis as seen in the lower part of Fig. 2.

3. Results and Discussion

3.1. Double-modulation double-resonance experiments

The mmw spectra were very dense and most of the lines measured at room temperature remained finally unassigned. We suspect that they belong to vibrational or torsional excited states. In the beginning, all assigned mmw lines were *R*-branch transitions. Torsional splittings due to the low barrier rotor typically ranged from a few MHz up to about 80 MHz. Splittings due to the higher barrier rotor remained unresolved. However, predictions performed by the program *XIAM* indicated that some *Q*-branch *b*-type transitions with splittings larger than 900 MHz for the low barrier and resolvable splittings for the high barrier rotor lie in the mmw region with low, yet detectable intensities. When attempting to measure these signals, we faced the problem that the mmw spectrum of 4MAP was too dense for a clear assignment. The DM-DR scheme was employed

to display the otherwise undetectable lines, see Fig. 2. We succeeded to record six *Q*-branch transitions with their fine structures. When assigning these signals, we found that the (12) symmetry species was missing from the spectrum (for the labelling, see Ref. [23]), despite the observation of all other symmetry species and the spin statistical weight stating that (12) should be as intense as (11) and half as intense as (10) [23]. Instead, the (10) and (11) species were found equally intense, as shown exemplarily in Fig. 2, indicating that either the frequency prediction is wrong and (11) and (12) are degenerated for these transitions, or, rather unlikely, the intensity predictions are wrong. In contrast *ERHAM* predicts the (11) and (12) lines to be degenerate, which is in agreement with our observations, and shows the superior predictive power of the *ERHAM* fits for these lines.

3.2. Fit performance

The different fitting methods used in this study reproduce the experimental spectrum with varying success. Following the procedure of starting with small datasets limited to microwave data with small quantum numbers and a small number of variables followed by sequentially increasing dataset and number of variables, we expect the fits to converge on global minima on the root-mean-square deviation hypersurface. This is supported by the small remnant deviations in our fits.

Local fits obtained with *SPFIT* achieve experimental accuracy. The global *ERHAM* fit performs slightly worse than the local fits but still shows satisfactory rms deviation. *XIAM* performs worse than *ERHAM* and fails to reproduce the spectrum to experimental accuracy, but still qualitatively catches most of its features. The input and output files of all fits are provided in the Supplementary Material.

The problems of the *XIAM* fits can be traced back to the lines showing the highest deviations. Except for the missing (12) lines of the transitions described under Section 3.1., initial fits carried out with *XIAM* could reproduce the frequencies of most transitions to experimental accuracy. Nevertheless, a few mmw lines, typically *R*-branch high *K* transitions, still remain with rather large deviations from 300 to 500 kHz. Also a few lines measured with the resonator in the microwave region show deviations of up to 104 kHz, in contradiction with the measurement accuracy being 5 kHz or better. It should be noted at this point, that even in the local fits with *SPFIT*, deviations in the resonator data of up to 16 kHz occur because of additional splittings or line broadening. Such splittings have been reported in previous studies on phenyl containing two-top molecules using the same setup [38,39] and are probably caused by spin-rotation coupling arising from the hydrogen atoms of the methyl rotors. This assumption is supported by the fact that the splittings or line-broadening are more pronounced for the A species lines with spins of the three hydrogens aligning $I_{\mathrm{H_3}} = 1.5$ compared to the E species with $I_{\mathrm{H_3}} = 0.5$. An example is given in Fig. 3.

3.3. Fit interpretation

We will now look at the interpretability of fit parameters and compare the local and global fits. We will see that results from local fits can be translated to structural rotational constants and energetic barriers. *ERHAM* and *ntop* provide significantly different rotational constants compared to *XIAM* and local fits carried out with *SPFIT*.

3.3.1. Local fits

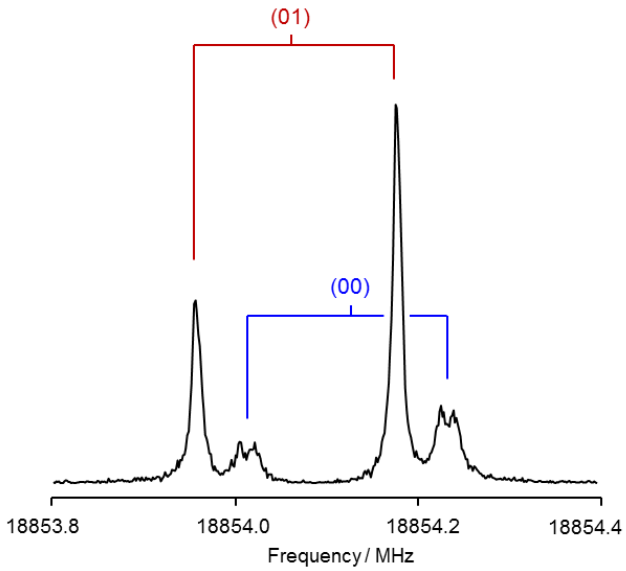

Figure 3. The $6_{24} - 5_{15}$ transition of 4MAP recorded using the COBRA spectrometer, showing that (i) the splitting between the (00) and (01) torsional species is well-resolved and (ii) additional splittings are observed for the (00) species. For this spectrum, 205 free induction decays were co-added. Due to the experimental geometry, transition signals appear as Doppler doublets.

Local fit parameters must be converted using Herschbach's perturbation coefficients for interpretation. The local rotational constants

$$B_{v\sigma} = B_v + W_{v\sigma}^{(2)} F \rho_{\mathrm{b}}^2 \qquad (3)$$

are related to the structural rotational constants B_v, the second order perturbation coefficients $W_{v\sigma}^{(2)}$, the reduced rotational constant F of the internal rotor, and the respective coupling vector component ρ_{b}. In some cases, similar to centrifugal distortion corrections when applying Watson's A or S reduction, higher order corrections should be taken into account. The magnitude of quartic centrifugal distortion coefficients in the local fits is an indication whether these corrections are required or not. In the case of 4MAP the largest coefficient is that of D_K = 58.10(5) kHz in the (10) species local fit. Based on this rather small value, we will neglect the higher order corrections.

For high barrier one-top cases, the approximation

$$W_{v\mathrm{A}}^{(2)} \approx -2W_{v\mathrm{E}}^{(2)} \qquad (4)$$

can be applied to derive the structural rotational constants B_v as a simple weighted average [40]:

$$B_0 = \frac{B_{0\mathrm{A}} + 2B_{0\mathrm{E}}}{3} \qquad (5)$$

where v = 0 and $B_{0\mathrm{A}}$ and $B_{0\mathrm{E}}$ are the rotational constants of the separate A and E species fits, respectively. The weighted average results in rotational constants comparable to those of the *XIAM* global fits. This is also found in the recent study of 2-acetylfuran [43] and can generally be found in other studies of high barrier rotors.

In 4MAP, the high barrier approximation has been applied to the higher barrier acetyl methyl rotor (V_3 = 580 cm^{-1}, s = 49) to reduce the five sets of rotational constants of the different species to two sets $B_{0\mathrm{A}}$ and $B_{0\mathrm{E}}$ related to the low barrier *para*-methyl rotor: $B_{0\mathrm{A}}$ was calculated as in Eq. (5) from $B_{0,(00)}$ and $B_{0,(01)}$. The $B_{0\mathrm{E}}$ was calculated by taking the mean average of the rotational constants of the (10), (11), and (12) species. This results in values of $A_{0\mathrm{A}}$ = 3694.35818(31) MHz, $B_{0\mathrm{A}}$ = 784.650163(60) MHz, $C_{0\mathrm{A}}$ = 650.443967 MHz for the "*A* species" of the low barrier rotor and $A_{0\mathrm{E}}$ = 3639.41162(48) MHz, $B_{0\mathrm{E}}$ = 784.641511(12) MHz, $C_{0\mathrm{E}}$ = 650.458506(11) MHz for the "E species".

For the low barrier *para*-methyl rotor (V_3 = 22 cm^{-1}, s = 1.77), the approximation given in Eq. (4) is no longer valid, and appropriate second order perturbation coefficients $W_{v\sigma}^{(2)}$ must be calculated when deriving the structural rotational constants. We computed a plot of $W_{v\sigma}^{(2)}$ in Fig. 4, which shows its dependence on the reduced barrier s.

Furthermore, local fit results are related to internal rotation parameters and structural rotational constants via the perturbation coefficients. Due to the C_s symmetry, the angle $\delta \triangleq \sphericalangle(\alpha, a)$ can directly be derived from the first order parameters D_a and D_b :

$$\delta = \arctan\left(\frac{-A_0 D_b}{B_0 D_a}\right). \qquad (6)$$

Solving Eq. (2) for $W_{v\sigma}^{(1)}$ gives the perturbation coefficients as:

$$W_{v\sigma}^{(1)} = \frac{F_0 D_a}{F \cos(\delta) A_0} \qquad (7)$$

where

$$F_0 = F \cdot r \quad \text{with} \quad r = 1 - \frac{\cos(\delta)^2 A_0 + \sin(\delta)^2 B_0}{F_0} \qquad (8)$$

is the structural rotational constant of the internal rotor.

The δ calculated from Eq. (6) can be inserted into Eq. (7) to obtain $W_{v\sigma}^{(1)}$, which in turn can be related to the reduced barrier s. Once s is known, the $W_{v\sigma}^{(2)}$ coefficient can be derived, and thus the structural rotational constants and F can be determined from Eq. (3). At this point, a vicious cycle is obviously involved: The unknown structural rotational constants A_0, B_0, C_0, F_0 and reduced rotational constant F of the internal rotor are derived from the reduced barrier s; but to derive s, Eq. (7) requires the ratio F_0/F and A_0 to be known.

An iterative procedure, starting with a guess of s and F_0, was formulated to solve this problem. There is some flexibility in choice of details regarding such iterative procedures, and different solutions to this problem can be found in studies of several molecules, with one example being N-acetyl-alanine N'-methylamide [44]. The specific scheme used for 4MAP is described in the supplementary material.

3.3.2. Global fits

In global fits with *ERHAM*, rotational constants and geometric angles from the fit output might be used directly. Though the barrier is not a fit parameter in *ERHAM*, the torsional energy difference $E_{v\mathrm{E}} - E_{v\mathrm{A}}$ and the F constant are provided in the output. They are related to zero order Herschbach coefficients as follows:

$$W_{v\mathrm{E}}^{(0)} - W_{v\mathrm{A}}^{(0)} = \frac{E_{v\mathrm{E}} - E_{v\mathrm{A}}}{F}. \qquad (9)$$

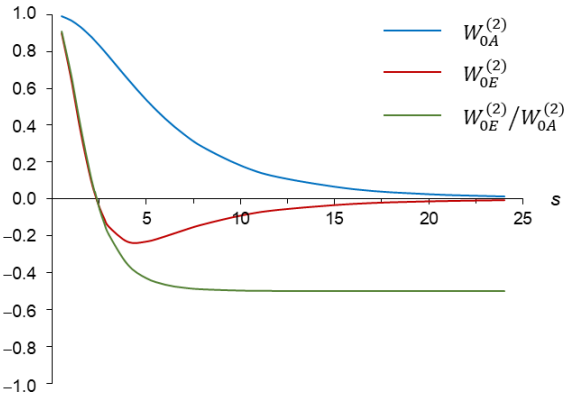

Figure 4. $W_{0\sigma}^{(2)}$ coefficients in dependence of the reduced barrier. At very small reduced barriers (say s < 5), significant deviations from the high barrier approximation $W_{0,\mathrm{E}}^{(2)}/W_{0,\mathrm{A}}^{(2)}$ = −0.5 occur.

The quantities in Eq. (9) can be related to the reduced barrier s. We used the *Mathieu* program, written by Wolfgang Stahl, for this purpose. That Eq. (9) is a possible method to derive barriers from *ERHAM* fits can be demonstrated for high barrier cases; for example, the recently studied propylene oxide in its first torsional excited state. In that study, a reduced barrier of 67.92 was determined with *XIAM*. Fits using *ERHAM* were also provided, giving an energy level splitting of −231 MHz and a F constant of 176 GHz, which results in s = 67.89 [45].

3.3.3. Fit comparison

The reduced barrier of 4MAP is provided in Tab. 1 along with the rotational constants $B_{\mathrm{g},0}$ and angles δ. Values obtained from different programs and from quantum chemical predictions are compared. Calculations were performed using the Coulomb-attenuating method, Becke, three-parameter, Lee-Yang-Parr functional [46] combined with Grimme's D3 dispersion corrections [47] and Becke-Johnson damping function BJ [48] at an aug-cc-pVTZ basis set (CAM-B3LYP-D3BJ/aug-cc-pVTZ), put to work in a geometry optimization with subsequent anharmonic frequency calculations as implemented in the *Gaussian 16* program package [49]. The combination of optimization with subsequent vibrational calculation was used to obtain ground state rotational constants $B_{\mathrm{g},0}$. The CAM-B3LYP-D3BJ/aug-cc-pVTZ method was chosen as it provided rotational constants with a typical accuracy of about 0.5% in previous structural determination studies [50].

The A_0 rotational constants obtained from the *XIAM* and *ntop* fits deviate significantly from the quantum chemically predicted value by 0.9% and 1.2% respectively. While these deviations might still be explainable with errors in the quantum chemical prediction method, they are large enough to question the plausibility of the results. It is stated in Ref. [5] that rotational constants obtained with *XIAM* can be interpreted as structural parameters, however, this statement has never been confirmed for low barrier cases. Therefore, we determined the structural constants of 4MAP from different (global and local) procedures to compare the results (see Tab. 1). Despite the very low torsional barrier of one methyl group in 4MAP, the rotational constants derived from *SPFIT* local fits agree qualitatively well with those from *XIAM* with deviations not exceeding 0.8 MHz. Such deviations might arise from the derivation process in the local fits. Also the F_0 constant of about 164 GHz derived from the local fits is somewhat too large, when it is

compared to the well-known value of 160 GHz found for unsubstituted toluene [51]. This might be due to model errors when assuming a pure threefold potential and no top-top interactions, leading to variations in the weight coefficients when deriving the structural rotational constants and F_0 from the local fits. In addition, none of the models considers a dependence of F on the torsional angle α, which might also contribute to the observed deviations between the methods, though such a dependence is expected to be small for the *para*-methylrotor of 4MAP. A rough estimate of $F(\alpha)$ can be obtained from relaxed potential energy surface scans [52]. Such rough estimates put the variation at about ±2.4 GHz and more details are provided in the supplementary material. Nevertheless, the agreement between local fits and *XIAM* supports the idea that *XIAM* provides structural rotational constants, while *ntop* does not.

The rotational constants obtained from *ERHAM* differ significantly from those derived from the local fits and *XIAM*. Contrary to *ntop*, these deviations are towards a larger A_0 constant. The parameter set used in *ERHAM* yields rotational constants following the high barrier approximation - nearly identical to those obtained with Eq. (5) when inserting rotational constants from *SPFIT* local fits. This suggests that for low barrier cases, rotational constants obtained from *ERHAM* are not to be used for structure determination purposes. The *para*-methyl barrier derived from the torsional energy difference and the F constant is also not in agreement with those derived from other methods, providing a somewhat smaller value of only s = 1.61 compared to 1.77 for *XIAM* and to 1.75 for local fits. Also, the derived F_0 constant is probably too large with a value of 169 GHz. The deviations for the low barrier rotor are likely a consequence of the effective nature of the parameters fitted, correlation problems, and the fact, that the internal rotation Hamiltonian is not solved explicitly in *ERHAM*. Low barriers in general might cause trouble, as mentioned by Groner in Ref. [20]. On the other hand, the results for the acetyl methyl rotor agree well with those of the other methods, as expected for a high barrier rotor. Despite the lack of interpretability with respect to the variables of the fit, *ERHAM* reaches almost experimental accuracy for the global data set with a performance that can be put between *XIAM* and local fits (the local fits provide somewhat more accurate reproductions of the experimental frequencies).

3.4. Fitting time

Regarding the usability of a program, the time required to carry out a fit when high quantum numbers are involved might be important. The bottleneck of the fitting procedure is the setting up and subsequent diagonalization of the matrix representations of the Hamiltonian. The highest J quantum number in the dataset (J_{max} = 91 in the case of 4MAP) reflects the time demand in fitting. For *ntop*, the calculations were too expensive. Therefore, we limit the use of *ntop* to fit the microwave data as published in Ref. [23]. *XIAM* succeeds to deal with such matrix sizes, but a fit typically requires up to a day. The local fits with *SPFIT* require only seconds and are as fast as *ERHAM*.

Conclusions

Two general approaches, global fits and local fits of each torsional species, were tested on the rotational data set with J_{max} = 91 of the two-top molecule 4MAP, featuring a high barrier (about 580 cm^{-1}) and a very low barrier (22 cm^{-1}) to methyl internal

Table 1. Rotational constants and internal rotation parameters as obtained from the *XIAM* and *ERHAM* fits as well as calculated at the CAM-B3LYP-D3BJ/aug-cc-pVTZ level of theory. Derived rotational constants from the local *SPFIT* fits are also summarized. 1-σ errors are given in parentheses. The program *PIFORM* [4] was used to derive 1-σ statistical errors of *SPFIT* parameters.

	global			local	Prediction
Parameter	*ntop*[a]	*ERHAM*[b]	*XIAM$_{mod}$*	*SPFIT*[c]	*Ab initio*
A_0 /MHz	3604.7132(19)	3657.72743(25)	3619.025(61)	3619.83674(66)	3650.2
B_0 /MHz	784.64659(30)	784.644311(34)	784.65137(18)	784.63843(16)	787.8
C_0 /MHz	650.43931(23)	650.453948(30)	650.44271(12)	650.46369(15)	653.6
$s_1 = 4V_{3,1}/9F_1$	1.7963323(2)	1.6125(56)	1.7722(22)	1.74642233(76)	1.49[d]
δ_1 /°	0.763225(57)	0.76494(33)	0.7648(11)	0.76261(49)	0.26[d]
$F_{0,1}$ /GHz	161.29(fixed)	168.7(11)	162.16(13)	163.9444(18)	161.29[d]
$s_2 = 4V_{3,2}/9F_2$	49.12(1)	49.43(13)	48.58(26)[e]	–	37.79[d]
δ_2 /°	123.0(32)	127.50(52)	129.2(13)	–	122.98[d]
$F_{0,2}$ /GHz	159.54(fixed)	162.2(22)	159.54(fixed)	–	159.54[d]
N_{par}[f]	19	26	22	7/8/15/10/10	
$N_{Res}/N_{CP}/N_{mmw}$[g]	0/88/0	579/335/350	579/335/350	579/335/350	
$\sigma_{Res}/\sigma_{CP}/\sigma_{mmw}$ /kHz[h]	–/26/–	4.1/32.6/65.5	25.7/38.0/80.0	3.8/33.4/33.2	
$\Delta_{max,Res}/_{CP}/_{mmw}$ /kHz[i]	–/88/–	30/100/305	104/112/463	16/115/138	
Time	–	Seconds	Hours	Seconds	

[a] Microwave data from Ref. [23].
[b] Barriers for *ERHAM* were determined from provided torsional energies and *F* constants.
[c] The V_6 term only has a small influence on the values derived purely from V_3 and F and is therefore neglected in the derivation from local fits.
[d] Internal rotation parameters taken from calculations at the B3LYP-D3BJ/def2TZVP level provided in Ref. [23].
[e] Note that this value is not the same as the value given by *XIAM*. There was a bug in the program when deriving the reduced barrier for the high barrier rotor. Therefore, we recalculated it from F and V_3.
[f] Number of fitted parameters. For the separate fits, the values given are for (00)/(01)/(10)/(11)/(12), respectively.
[g] Number of COBRA/chirped-pulse/millimeter-wave transitions. The total number of assigned transitions is 1264, but only 1078 frequencies of lines are determined due to degeneracy of some transitions.
[h] Root-mean-square (*rms*) deviation of COBRA/chirped-pulse/millimeter-wave lines.
[i] Maximum deviation of COBRA/chirped-pulse/millimeter-wave lines.

rotation. Based on the results summarized in Tab. 1, it is highly recommended to use both approaches when assigning spectra of molecules with low-barrier methyl torsion. Deviations in the fits can hint towards errors and is of great help in assigning rotational spectra. At least, this was the case when we investigated 4MAP.

If a reasonable *XIAM* fit is achievable, the rotational constants derived from *XIAM* are reliable for structure determination purposes, even though the *rms* deviation is not quite within the measurement accuracy. *SPFIT* local fits reached experimental accuracy and *ERHAM* reached almost experimental accuracy. Regarding the interpretability of the parameters, however, deriving physically meaningful parameters from local fits is a tedious task. When done correctly, they can still be useful. For *ERHAM*, the rotational constants and low barrier rotor parameters are not rationalized by a physical model compared to the other procedures. They deviate so much in fact, that we suggest considering *ERHAM* only for spectral fitting and predictions, and not for interpretations in terms of structure determinations or barrier comparisons, if low barriers are present. For the higher barrier, the local fits show problems that arise because D_b is not determined, thus prohibiting derivation of internal rotation parameters without additional assumptions. The program *ntop* provides experimental accuracy fits for small datasets, but requires unaffordable computation times when large quantum numbers are involved. In addition, the A_0 rotational constant provided by *ntop* for 4MAP is in strong disagreement with all other methods and the quantum chemical predictions. This implies that *ntop* does not provide structural rotational constants, at least when low barrier rotors are present.

Finally, we suggest testing these conclusions in a structure determination study involving isotopic substitutions using either 4MAP or a similar molecule. The time demand of such a study will be large, since it will be required to fit more than just the three rotational constants for each substitution. Also internal rotation parameters must be fit for each isotopologue independently, demanding for large data sets. From a computational point of view, the rotational constants of each isotopologue must then be corrected from experimental vibrational ground state constants to equilibrium constants. The supplemented fit files will be of help in approaching such study.

Acknowledgements

The measurements in Cologne are carried out within the Collaborative Research Centre 956 (project ID 184018867), sub-projects B3 and B4 and the “Cologne Center for Terahertz Spectroscopy” (project ID SCHL 341/15-1), funded by the Deutsche Forschungsgemeinschaft (DFG). B.H. and N.W. acknowledge financial support by the DFG under project ID WE 5874/1-1. H.V.L.N. is supported by the Agence Nationale de la Recherche ANR (project ID ANR-18-CE29-0011). Computations were supported by the cluster system team at the Leibniz University IT services (LUIS) Hannover, Germany.

Supplementary material

The supplementary information contains inputs and outputs of all fits, a description of the applied iteration scheme to derive parameters from local fits, and details on estimations of $F_0(\alpha)$. Also the input and output files of the anharmonic frequency calculations with Gaussian16 are provided.

Data availability statement

The data that supports the findings of this study are available within the article and its supplementary material. The program *Mathieu* written by Wolfgang Stahl is available with S.H. and H.V.L.N.

Authors Declarations

The authors have no conflicts to disclose.

References

[1] H. V. L. Nguyen, I. Kleiner, in: I. Gulaczyk, B. Tylkowski (Eds.), *Theoretical and computational chemistry*, De Gruyter, 2021, pp. 41-52, DOI: 10.1515/9783110678215-002

[2]. I. Kleiner, *J. Mol. Spectrosc.,* **260**, 1-18 (2010), DOI: 10.1016/j.jms.2009.12.011

[3] C. C. Lin, J. D. Swalen, *Rev. Mod. Phys.* **31**, 841-892 (1959), DOI : 10.1103/RevModPhys.31.841

[4] Z. Kisiel, in: J. Demaison et al. (Eds.), *Spectroscopy from Space,* Kluwer Academic Publishers, Dordrecht, 2001, pp.91-106, http://info.ifpan.edu.pl/~kisiel/prospe.htm.

[5] H. Hartwig, H. Dreizler, *Z. Naturforsch., A: Phys. Sci*., **51a**, 923–932 (1996), DOI: 10.1515/zna-1996-0807.

[6] P. Groner, *J. Chem. Phys.,* **107**, 4483-4498 (1997), DOI: 10.1063/1.474810

[7] J. T. Hougen, I. Kleiner, M. Godefroid, *J. Mol. Spectrosc*., **163**, 559-586 (1994) DOI: 10.1006/jmsp.1994.1047.

[8] I. Kleiner and J. T. Hougen, *J. Chem. Phys.* **119**, 5505-5509 (2003) DOI: 10.1063/1.1599354

[9] M. Tudorie, I. Kleiner, J. T. Hougen, S. Melandri, L. W. Sutikdja, W. Stahl, *J. Mol. Spectrosc.* **269**, 211-225 (2011) DOI: 10.1016/j.jms.2011.07.005

[10] V. V. Ilyushin, Z. Kisiel, L. Pszczółkowski, H. Mäder, J. T. Hougen, *J. Mol. Spectrosc.* **259**, 26-38 (2010) DOI: 10.1016/j.jms.2009.10.005

[11] V. V. Ilyushin and J. T. Hougen, *J. Mol. Spectrosc.* **289**, 41-49 (2013), DOI: 10.1016/j.jms.2013.05.012

[12] N. Ohashi and J. T. Hougen, *J. Mol. Spectrosc.* **203**, 170-174 (2000) DOI: 10.1006/jmsp.2000.8153

[13] L. Ferres, W. Stahl, H. V. L. Nguyen, *J. Chem. Phys.* **148**, 124304 (2018), DOI : 10.1063/1.5016273

[14] L. Ferres, W. Stahl, H. V. L. Nguyen, *J. Chem. Phys.* **151**, 104310 (2019), DOI: 10.1063/1.5116304

[15] V. Van, T. Nguyen, W. Stahl, H. V. L. Nguyen, I. Kleiner, *J. Mol. Struct.* **1207**, 127787 (2020), DOI: 10.1016/j.molstruc.2020.127787

[16] H. M. Pickett, *J. Chem. Phys.*, **107**, 6732–6735 (1997) DOI: 10.1063/1.474916

[17] H. M. Pickett, *J. Mol. Spectrosc.,* **148**, 371–377 (1991), DOI: 10.1016/0022-2852(91)90393-O

[18] R. C. Woods, *J. Mol. Spectrosc*., **21**, 4–24, (1966) DOI: 10.1016/0022-2852(66)90117-2

[19] R. C. Woods, *J. Mol. Spectrosc*., **22**, 49–59, (1967) DOI: 10.1016/0022-2852(67)90147-6.

[20] P. Groner, *J. Mol. Spectrosc.,* **278**, 52-67 (2012) DOI: 10.1016/j.jms.2012.06.006

[21] B. J. Drouin, J. C. Pearson, A. Walters, V. Lattanzi, *J. Mol. Spectrosc.* **240**, 227-237 (2006), DOI: 10.1016/j.jms.2006.10.007

[22] D. R. Herschbach, **31**, 91-108 (1959), DOI: 10.1063/1.1730343

[23] S. Herbers, S. M. Fritz, P. Mishra , H. V. L. Nguyen , T. S. Zwier, *J. Chem. Phys.* **152**, 074301 (2020), DOI: 10.1063/1.5142401

[24] L. H. Xu, J. T. Hougen*, J. Mol. Spectrosc.* 173, 540-551 (1995), DOI: 10.1006/jmsp.1995.1255
[25] I. Kleiner, *ACS Earth Space Chem.* **3**, 1812−1842 (2019) DOI: 10.1021/acsearthspacechem.9b00079
[26] K. Eibl, W. Stahl, I. Kleiner, H. V. L. Nguyen, *J. Chem. Phys.* **149**, 144306 (2018) DOI: 10.1063/1.5044542
[27] Y. Zhao, W. Stahl, H. V. L. Nguyen*, Chem. Phys. Lett.,* **545**, 9-13 (2012) DOI: 10.1016/j.cplett.2012.07.009
[28] L. Ferres, K.-N. Truong, W. Stahl, H. V. L. Nguyen, *ChemPhysChem* **19**, 1781-1788 (2018), DOI: 10.1002/cphc.201800115
[29] C. J. Smith, A. K. Huff, H. Zhang, Y. Mo , K. R. Leopold , *J. Chem. Phys.* **150**, 134302 (2019), DOI: 10.1063/1.5087718
[30] K. P. R. Nair, S. Herbers, A. Lesarri, J.-U. Grabow, *J. Mol. Spectrosc.*, **361,** 1-7 (2019), DOI: 10.1016/j.jms.2019.05.003
[31] S. Herbers, H. V. L. Nguyen, *J. Mol. Spectrosc.* **370**, 111289 (2020), DOI: 10.1016/j.jms.2020.111289
[32] K. P. R. Nair, S. Herbers, H. V. L. Nguyen, J.-U. Grabow, *Spectrochim. Acta A* **242**, 118709 (2020), DOI: 10.1016/j.saa.2020.118709
[33] M. Hermanns, N. Wehres, F. Lewen, H. S. P. Müller, S. Schlemmer, *J. Mol. Spectrosc.,* **358**, 25–36 (2019), DOI: 10.1016/j.jms.2018.11.009
[34] J.-U. Grabow, W. Stahl, H. Dreizler, *Rev. Sci. Instrum*. **67**, 4072-4084 (1996), DOI: 10.1063/1.1147553
[35] M. H. Ordu, O. Zingsheim, A. Belloche, F. Lewen, R. T. Garrod, K. M. Menten, S. Schlemmer, H. S. P. Müller, *A&A*, **629**, A72 (2019), DOI : 10.1051/0004-6361/201935887
[36] M.-A. Martin-Drumel, J. van Wijngaarden, O. Zingsheim, F. Lewen, M. E. Harding, S. Schlemmer, S. Thorwirth, *J. Mol. Spectrosc.,* **307**, 33-39 (2015), DOI : 10.1016/j.jms.2014.11.007
[37] O. Zingsheim, L. Bonah, F. Lewen, S. Thorwirth, H. S. P. Müller, S. Schlemmer,*J. Mol. Spectrosc.,* **381**, 111519 (2021), DOI: 10.1016/j.jms.2021.111519
[38] J. Mélan, S. Khemissi, H. V. L. Nguyen, *Spectrochim. Acta A* **253**, 119564 (2021), DOI: 10.1016/j.saa.2021.119564
[39] S. Khemissi, H. V. L. Nguyen, *ChemPhysChem* **21**, 1682-1687 (2020), DOI: 10.1002/cphc.202000419
[40] Gordy, W., Cook, R. L. *Microwave Molecular Spectra*, Equations 12.52 and 12.56, Vol. **18**, 3rd Ed., Wiley: New York, USA, (1984).
[43] C. Dindić, A. Lüchow, N. Vogt, J. Demaison, H.V.L. Nguyen, *J. Phys. Chem. A* **125**, 4986−4997 (2021), DOI: 10.1021/acs.jpca.1c01733
[44] R. J. Lavrich, D. F. Plusquellic, R. D. Suenram, G. T. Frase, A. R. Hight Walker, M. J. Tubergen*, J. Chem. Phys.* **118**, 1253-1265 (2003), DOI: 10.1063/1.1528898
[45] P. Stahl, B. E. Arenas, O. Zingsheim, M. Schnell, L. Margulès, R. A. Motiyenko, G. W. Fuchs, T. F. Giesen, *J. Mol. Spectrosc.* **378**, 111445 (2021), DOI: 10.1016/j.jms.2021.111445
[46] T. Yanai, D. P. Tew, N. C. Handy, *Chem. Phys. Lett.* **393**, 51–57 (2004). DOI: 10.1016/j.cplett.2004.06.011
[47] S. Grimme, J. Antony, S. Ehrlich, H. Krieg, *J. Chem. Phys*. **132**, 154104 (2010), DOI: 10.1063/1.3382344
[48] E. R. Johnson, A. D. Becke, *J. Chem. Phys.* 123, 024101 (2005), DOI: 10.1063/1.1949201
[49] M. J. Frisch, G. W. Trucks, H. B. Schlegel, G. E. Scuseria, M. A. Robb, J. R. Cheeseman, G. Scalmani, V. Barone, G. A. Petersson, H. Nakatsuji, X. Li, M. Caricato, A. V. Marenich, J. Bloino, B. G. Janesko, R. Gomperts, B. Mennucci, H. P. Hratchian, J. V. Ortiz, A. F. Izmaylov, J. L. Sonnenberg, D. Williams-Young, F. Ding, F. Lipparini, F. Egidi, J. Goings, B. Peng, A. Petrone, T. Henderson, D. Ranasinghe, V. G. Zakrzewski, J. Gao, N. Rega, G. Zheng, W. Liang, M. Hada, M. Ehara, K. Toyota, R. Fukuda, J. Hasegawa, M. Ishida, T. Nakajima, Y. Honda, O. Kitao, H. Nakai, T. Vreven, K. Throssell, J. A. Montgomery, Jr., J. E. Peralta, F. Ogliaro, M. J. Bearpark, J. J. Heyd, E. N. Brothers, K. N. Kudin, V. N. Staroverov, T. A. Keith, R. Kobayashi, J. Normand, K. Raghavachari, A. P. Rendell, J. C. Burant, S. S. Iyengar, J. Tomasi, M. Cossi, J. M. Millam, M. Klene, C. Adamo, R. Cammi, J. W. Ochterski, R. L. Martin, K. Morokuma, O. Farkas, J. B. Foresman, and D. J. Fox, GAUSSIAN 16 Revision B.01, Gaussian, Inc., Wallingford, CT, 2017.
[50] S. Herbers, P. Kraus, J.-U. Grabow, *J. Chem. Phys.* **150**, 144308 (2019), DOI: 10.1063/1.5091693
[51] V. V. Ilyushin, E. A. Alekseev, Z. Kisiel, L. Pszczółkowski, *J. Mol. Spectrosc.* 339, 31-39 (2017), DOI: 10.1016/j.jms.2017.01.005
[52] D. Tikhonov, ChemRxiv. Cambridge: Cambridge Open Engage (2021) DOI: 10.33774/chemrxiv-2021-v74sm-v3